Optimized *E*-Plane T-Junction Series Power Dividers

FRITZ ARNDT, SENIOR MEMBER, IEEE, INGO AHRENS, UWE PAPZINER, ULRICH WIECHMANN, AND REINHARD WILKEIT

Abstract—**A rigorous design theory for compact rectangular waveguide power dividers with unsymmetrical series *E*-plane T-junctions of suitably optimized different waveguide heights and distances is described. The method is based on field expansion in normalized eigenmodes which yield directly the modal *S*-matrix of two appropriate key building blocks. The immediate modal *S*-matrix combination of the individual structures includes the effects of all step discontinuities and their mutual higher order mode interaction. Computer-optimized −3.01 dB, −4.77 dB, and −6.02 dB power divider examples achieve about ±0.25 dB coupling deviation at the output ports, together with about 30 dB return loss at the input port, for the chosen design frequencies of 12 GHz, 31.6 GHz, and 15.5 GHz. The −4.77 dB power divider provides a bandwidth of about 8 percent. The theory is verified by measurements.**

I. Introduction

WAVEGUIDE SYSTEMS for satellite communication applications require simple low-insertion-loss components which are appropriate for compact topology and are as light as practicable. Therefore, the old principle of direct power splitting by waveguide *E*-plane T-junction [1] series configurations—also known as "squintless feeds" [2]—has found new interest for all applications in satellite microwave systems [3], [4], where size, weight, and simplicity are critical design factors and where the typical shortcoming inherent in such three-port elements, i.e., poor isolation between the output ports, is of less importance. *E*-plane junctions allow convenient milling and spark eroding techniques from a solid block, which produces waveguide channels of identical *a*-dimension milling depth (i.e., identical fundamental-mode cutoff frequency); the waveguide heights may simply be modified appropriately for impedance matching purposes. Moreover, *E*-plane power dividers are highly compatible with printed *E*-plane components [5], [6] such as diplexers [5], [7], which are of growing interest in recent millimeter-wave circuit designs.

Available analysis methods for single *E*-plane T-junctions [1], [8]–[12] do not include the influence of three unequal waveguide branches. The approximation of unsymmetrical T-junctions by an average reference plane, as suggested in [20], [8], and [9] for branch-guide couplers, is inadequate for the optimum design of T-junction series power dividers. This is because the effects of both the magnitude and the phase caused by each individual step discontinuity of the unequal branch heights are utilized directly for controlling the ratio of the power division, as well as for compensating the frequency response at the ports. Moreover, the higher order mode coupling effect of series T-junction discontinuities has been neglected in previous designs. The purpose of this paper, therefore, is to describe a computer-aided design method for unsymmetrical *E*-plane T-junction series power dividers (Fig. 1) which takes these effects rigorously into account. The structure requires no additional matching elements, and the desired power divider performance may be achieved by suitably designing the unsymmetrical branch heights and the T-junction distances (Fig. 1(a), (b)). Although the two design types (Fig. 1(a), (b)) show similar power division properties, the back-step tapered power divider type (Fig. 1(b)) has turned out to achieve better input VSWR behavior than its counterpart (Fig. 1(a)).

The design method is based on field expansion into normalized incident and scattered waves [10]–[14]. The principle of expansion of electromagnetic fields in cavities [17], [12] is utilized, which yields, for this kind of discontinuity, rapidly converging expansion functions and allows the multiaperture problem to be reduced to a mere superimposition of simpler cavity problems by subsequently shorting all apertures but one. The theory yields directly the modal scattering matrix of the waveguide discontinuity under consideration. The immediate modal *S*-matrix combination of all interacting structures includes the effects of all discontinuities and their mutual higher order mode coupling. Moreover, this technique of direct *S*-matrix combination preserves numerical accuracy and requires no symmetry of ports or modes of the individual waveguide elements to be combined.

An appropriate admittance matrix formulation may provide, if desired, easy-to-apply equivalent circuit parameters [1] based on the accurate field theory modal *S*-matrix method given. This allows well-established simple network theory methods [1], [8], [9] to be applied as well. However, the restricted validity of this approach is demonstrated for a symmetrical T-junction example.

The field theory computer-aided design method presented is verified by optimized power divider examples with power division in equal parts. Data for optimized power dividers with two T-junctions (division in three parts, i.e., −4.77 dB coupling) are given for R140 (15.8

Manuscript received September 16, 1986; revised May 18, 1987. This work was supported by MBB/Erno Raumfahrt GmbH., München, West Germany.

The authors are with the Microwave Department, University of Bremen, NW1, D-2800 Bremen 33, West Germany.

IEEE Log Number 8716590.

0018-9480/87/1100-1052$01.00 ©1987 IEEE

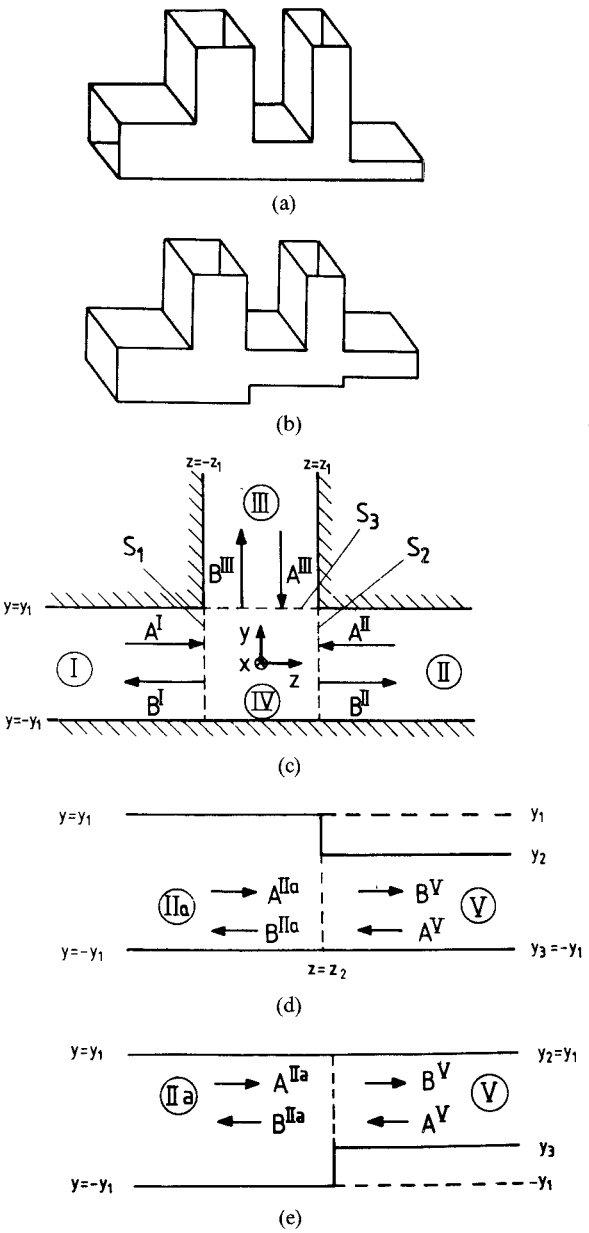

Fig. 1. Unsymmetrical *E*-plane T-junction series power divider. (a) Top-step tapered type. (b) Back-step tapered type. (c) Subregions for the T-junction discontinuity. (d) Subregions for the discontinuity step in height (top-step type). (e) Subregions for the discontinuity step in height (back-step type).

mm×7.9 mm), R220 (10.7 mm×4.3 mm), and R320 (7.1 mm×3.55 mm) input waveguides. Optimized power dividers with three T-junctions (division in four parts, i.e., −6.02 dB coupling) and four T-junctions (division in five parts, i.e., −6.99 dB coupling) are presented for the R140 input waveguide. Measured results for a two-T-junction power divider show good agreement with the theoretically predicted values.

II. Theory

The coupling section of the unsymmetrical T-junctions with unequal branch heights (Fig. 1(a), (b)) is decomposed into two key building blocks, the symmetrical T-junction with arbitrary branch height $2z_1$ and equal heights $2y_1$ in the main waveguide (Fig. 1(c)), and the discontinuity change in waveguide height (Fig. 1(d), or (e), respectively). The total scattering matrix of the unsymmetrical T-junction is formulated by suitable direct combination of the related individual modal scattering matrices.

A TE_{10} wave incident in port I (Fig. 1(c)) excites longitudinal section TE^x_{1n} waves [13], [15]. Therefore, for each typical homogeneous subregion $v = $ I, II, III (Fig. 1(c)), and $v = $ IIa, V (Fig. 1(d), (e)) the fields, [15], [16]

$$\vec{E}^{(v)} = -j\omega\mu\nabla\times\vec{\Pi}^{(v)}_{hx} \qquad \vec{H}^{(v)} = \nabla\times\nabla\times\vec{\Pi}^{(v)}_{hx} \quad (1)$$

are derived from the x component of the Hertzian vector potential $\vec{\Pi}_h$, which is assumed to be a sum of suitably normalized eigenmodes satisfying the vector Helmholtz equation and the corresponding boundary conditions:

$$\Pi^{(v)}_{hx} = \frac{2}{\sqrt{a(q_2-q_1)^{(v)}}}\,\frac{1}{\sqrt{k^2-k_x^2}}\cdot\sin(k_x x)\cdot\sum_{n=0}^{N}\left[\frac{1}{\sqrt{Z^{(v)}_{Fn}}}\cdot\frac{1}{\beta^{(v)}_n}\cdot\frac{1}{\sqrt{1+\delta_{0n}}}\cdot\cos\left(k^{(v)}_{qn}\left(t-q_1^{(v)}\right)\right)\right]\cdot\left[A^{(v)}_n e^{\mp j\beta^{(v)}_n s}-B^{(v)}_n e^{\pm j\beta^{(v)}_n s}\right]. \quad (2)$$

Here, a = waveguide width and $(q_2-q_1)^{(v)} = b^{(v)} =$ waveguide height in the corresponding subregion, i.e., y_1+y_1, z_1+z_1, or y_2-y_3, respectively. In addition,

$$k^2=\omega^2\mu\epsilon \qquad k_x=\frac{\pi}{a} \qquad Z^{(v)}_{Fn}=\frac{\omega\mu}{\beta^{(v)}_n}$$

$$k^{(v)}_{qn}=\frac{n\pi}{b^{(v)}} \qquad \delta_{0n}=\text{Kronecker delta}$$

$$\beta^{(v)}_n=\begin{cases}\sqrt{\omega^2\mu\epsilon-\left(k_x^2+k^{(v)2}_{qn}\right)} & \omega^2\mu\epsilon\geqslant k_x^2+k^{(v)2}_{qn}\\ -j\sqrt{\left(k_x^2+k^{(v)2}_{qn}\right)-\omega^2\mu\epsilon} & \omega^2\mu\epsilon\leqslant k_x^2+k^{(v)2}_{qn}\end{cases}$$

and t = position variable directed towards the waveguide height, i.e., y or z, respectively, and s = variable of the corresponding wave propagation, i.e., z or y, respectively. Note that the usual signs for the forward and backward wave amplitudes (i.e., the upper signs of the exponential function in (2)) correspond to the reference coordinate system indicated in Fig. 1(c). The related signs need to be interchanged for an inverse reference axis, e.g. for a T-junction opened in the $-y$ direction.

The eigenmodes in (2) with the still unknown amplitude coefficients A_n and B_n are suitably normalized, so that the power carried by a given wave is 1 W for a wave amplitude coefficient of $1\sqrt{W}$ [15].

The *modal scattering matrix of the symmetrical T-junction* is derived by extending the mode-matching procedure for a right-angle waveguide corner [12]. The field in the cavity subregion IV (Fig. 1(c)) is superimposed by three suitably

chosen standing wave solutions:

$$\Pi_{hx}^{IV} = \Pi_{hx}^{IV(1)} + \Pi_{hx}^{IV(2)} + \Pi_{hx}^{IV(3)} \tag{3}$$

where solution (1) is obtained if the boundary planes S_2 and S_3 (Fig. 1(c)) are short-circuited and S_1 is open; solutions (2) and (3) are found analogously [12]. Note, however, that the TE_{1n}^{x} formulation, (1) and (2), is different from [12]. This formulation advantageously requires only one vector potential component to be considered, instead of two [12].

By matching the tangential field components given by (1)–(3) at the common interfaces across the discontinuities $z = -z_1$, $y \in (-y_1, y_1)$, $z = z_1$, $y \in (-y_1, y_1)$, and $y = y_1$, $z \in (-z_1, z_1)$, respectively (Fig. 1(c)) and utilizing the orthogonal property of the modes [15], [16], the still unknown amplitude coefficients can be related to each other in the form of the desired scattering matrix of the symmetrical T-junction:

$$(B) = (S^T)(A) \tag{4}$$

where the matrix elements are elucidated in the Appendix.

The *modal scattering matrix of the discontinuity change in waveguide height* (Fig. 1(d), (e)) is calculated by direct mode matching of the tangential field components given by (1) and (2) at the common interfaces across the discontinuities at $z = z_2$. In order to include both types under consideration (Fig. 1(d), (e)), it is convenient to utilize the formulation for the more general discontinuity change from waveguide height $(y_1 - y_0)$ to $(y_2 - y_3)$, and to choose $y_3 = y_0$ for the case in Fig. 1(d), and $y_2 = y_1$ for the case in Fig. 1(e), respectively. Note further that for a discontinuity from lower to higher waveguide, only the port designations have to be interchanged. The wave amplitude coefficients are related to each other by the desired scattering matrix

$$(B) = (S^H)(A) \tag{5}$$

where the matrix elements are given in the Appendix.

The total *modal scattering matrix of the unsymmetrical T-junction*

$$(B) = (S^{UT})(A) \tag{6}$$

is given by suitably combining the related three-port matrix (S^T) with the two-port matrix (S^H), as described in [18]. For completeness, the equations are given in the Appendix using the present notation. The overall modal scattering matrix of the complete power divider structure is found by using this formulation iteratively, and by including the two-port scattering matrix of a homogeneous waveguide section for an appropriate consideration of the distances between the individual discontinuities. This procedure preserves numerical accuracy, avoids instabilities, and requires no symmetry of ports and modes [18].

For computer optimization, the expansion into ten eigenmodes at each step discontinuity and four eigenmodes along each intermediate homogeneous waveguide section has turned out to yield sufficient asymptotic behavior of the scattering coefficients. The final design data are provided by expansion into 18 eigenmodes.

For derivating an *equivalent-circuit representation*, the admittance matrix (Y) of the structure under consideration is calculated by

$$(Y) = (Y_0^D)^{1/2} \cdot (\bar{Y}) \cdot (Y_0^D)^{1/2} \tag{7}$$

with the normalized admittance matrix

$$(\bar{Y}) = [(U) + (S)]^{-1} \cdot [(U) - (S)].$$

(S) is the related scattering matrix of the single or composed structure calculated by the field theory presented; $(Y_0^D)^{1/2}$ is the diagonal matrix of the square root of the wave admittances $Y_{0i} = 1/Z_{F_i}$ (cf. (2)) in each of the ports i of the multiport under consideration; and (U) is the unit matrix. The network elements of a suitably chosen equivalent circuit may then be calculated by comparison of the related Y-matrices. For example, the simple equivalent-circuit parameters according to [1] for the symmetrical T-junction (cf. Fig. 2) are derivated by the Y-matrix elements using the expressions given in the Appendix.

III. Design

As has already been shown for optimized waveguide transformers [14] or couplers [13], the computer-aided design is carried out by a modified direct search method, the evolution strategy method [19], where the parameters of the error function are varied statistically. The advantages are such that local minima may be avoided and no differentiation step is necessary. An error function to be minimized is defined

$$F(\bar{x}) = \sum_{j=1}^{J} \left(\frac{S_{11}(f_j)}{S_{11D}} \right)^2 + \left(\frac{S_{21D}}{S_{21}(f_j)} \right)^2 + \left(\frac{S_{31D}}{S_{31}(f_j)} \right)^2 + \left(\frac{S_{41D}}{S_{41}(f_j)} \right)^2 + \cdots \stackrel{!}{=} \text{Min} \tag{8}$$

where J is the number of frequency sample points; S_{11D}, S_{i1D} are the desired given input reflection and corresponding transmission coefficients to the ports i; and $S_{11}(f_j)$ and $S_{i1}(f_j)$ are the calculated scattering coefficients at the frequency f_j. For given waveguide width a and number of output ports desired, the parameters $\bar{x}$ to be optimized (Fig. 1(a), (b)) are the distance of the T-junctions and the waveguide heights in all ports except the input port. The optimization program achieves the design of power dividers with up to five series T-junctions.

IV. Results

Fig. 2 shows the equivalent-circuit parameters, according to [1], for a symmetrical T-junction as a function of frequency. For low frequencies and for side arm height b' equal to the main line height b (Fig. 2(a)), the results of [1] agree relatively well with the values calculated with the rigorous field theory method described. For higher frequencies and for larger ratios b'/b (Fig. 2(b)), however, a significant deviation between the rigorous theory and [1] may be stated. For still higher frequencies (Fig. 2(c)), the

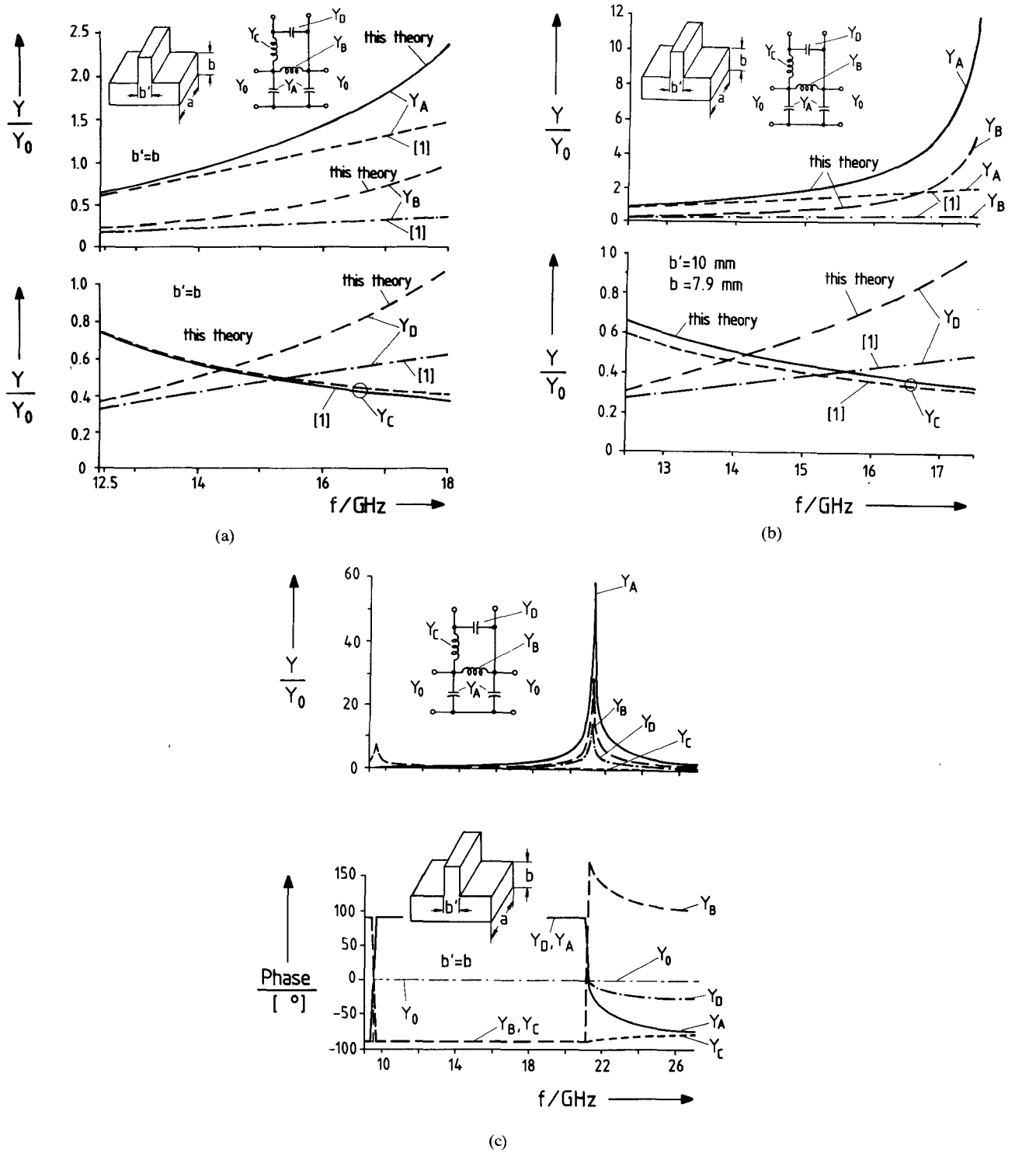

Fig. 2. Equivalent-circuit parameters. Comparison between field theory results, (1)–(7), and the results of Marcuvitz [1]. Waveguide dimensions $a = 15.8$ mm, $b = a/2$. (a) Ratio of the side arm height to main line height $b'/b = 1$. (b) $b'/b > 1$, $b' = 10$ mm. (c) Demonstration of the frequency range of validity, $b'/b = 1$.

equivalent-circuit parameter representation of the junction is degraded by the higher order mode propagation within the waveguide elements.

Fig. 3 compares the results of our method with available field theory results [11] for a symmetric T-junction. Very good agreement can be stated.

Although the two types of unsymmetrical T-junctions (Fig. 1(a), (b)) considered in the theory yield nearly equivalent power division properties, the back-step tapered type (Fig. 1(b)) achieves better input VSWR behavior. This type is preferred, therefore, for the demonstration of numerical examples. Further, the theory is verified by optimized power dividers with power division in equal parts. For other power levels desired, only the corresponding transmission coefficients S_{i1D} in (8) need to be chosen adequately.

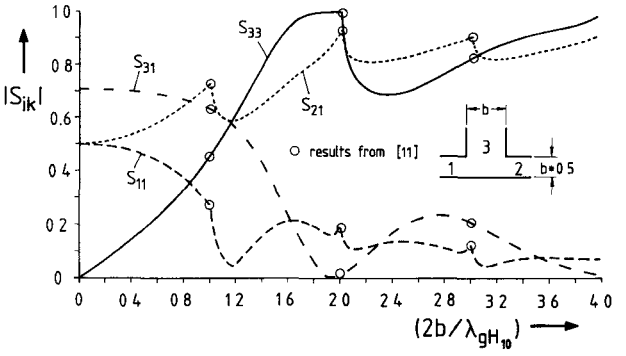

Fig. 3. Symmetrical E-plane T-junction. Magnitude of the scattering coefficients as a function of normalized frequency. Waveguide dimensions: $a = 2b$.

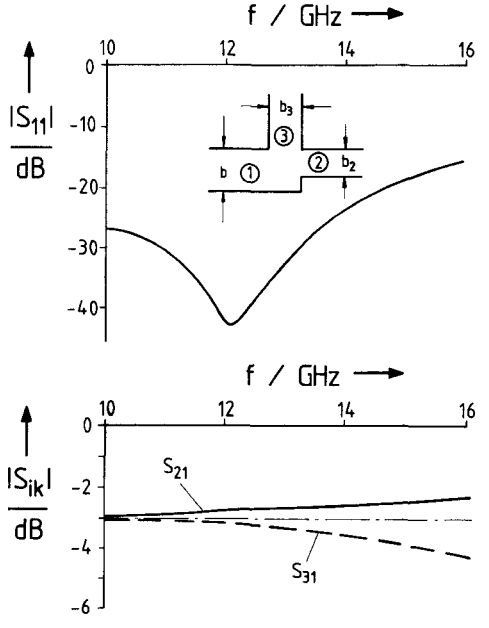

Fig. 4. E-plane T-junction with optimized different waveguide heights. Magnitude of the scattering coefficients in decibels as a function of frequency. Waveguide dimensions: $a = 2b = 15.799$ mm (R140-band); $b_2 = 4.41$ mm; $b_3 = 4.38$ mm.

The simple unsymmetric T-junction (Fig. 4) with suitably optimized waveguide heights of the output ports achieves $-(3.01 \pm 0.25)$ dB coupling to ports 3 and 2 together with more than 43 dB return loss at 12 GHz, as is demonstrated in Fig. 4 for an R140 input waveguide.

A relatively broad-band -4.77 dB design achieved by a series connection of two T-junctions with suitably optimized dimensions is shown in Fig. 5 for a R320-band example. Here $-(4.77 \pm 0.25)$ dB power division is provided for a bandwidth of about 2.5 GHz together with more than 36 dB return loss. Further design data for such power dividers in three ports, with similar characteristics but for the R140- and R220-waveguide band, respectively, are given in the caption to Fig. 5.

Power dividers of smaller bandwidth in four and five ports, with three and four series T-junctions, respectively, are shown in Figs. 6 and 7 for R140-waveguide-band examples. A $-(6.02 \pm 0.2)$ dB coupling is achieved at about 15.5 GHz for the four-series-T-junction design, to-

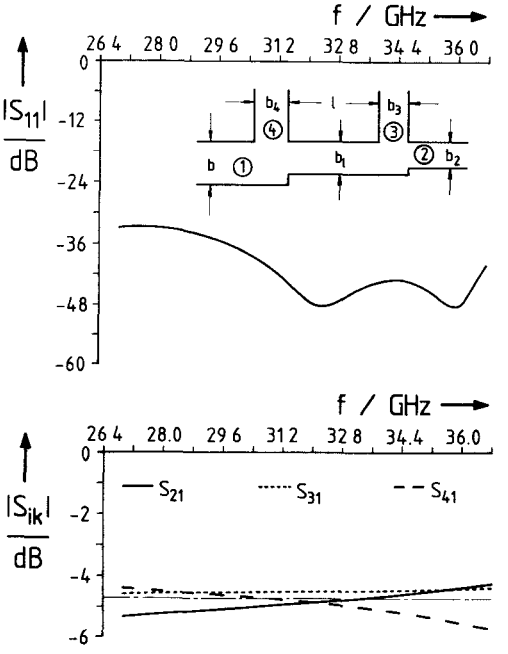

Fig. 5. Two series T-junctions with optimized waveguide heights and distance. Magnitude of the scattering coefficients in decibels as a function of frequency. Waveguide dimensions: $a = 2b = 7.112$ mm (R320-band); $b_2 = 1.26$ mm; $b_3 = 1.61$ mm; $l = 5.12$ mm; $b_1 = 2.54$ mm; $b_4 = 1.50$ mm. (The dimensions for respectively, a R140-band and an R220-band example are $a = 2b = 15.799$ mm, $b_2 = 2.98$ mm, $b_3 = 2.83$ mm, $l = 27.42$ mm, $b_1 = 5.43$ mm, $b_4 = 3.95$ mm, and $a = 10.668$ mm, $b = 4.318$ mm, $b_2 = 2.87$ mm, $b_3 = 3.39$ mm, $l = 1.93$ mm, $b_1 = 4.33$ mm, $b_4 = 2.92$ mm.)

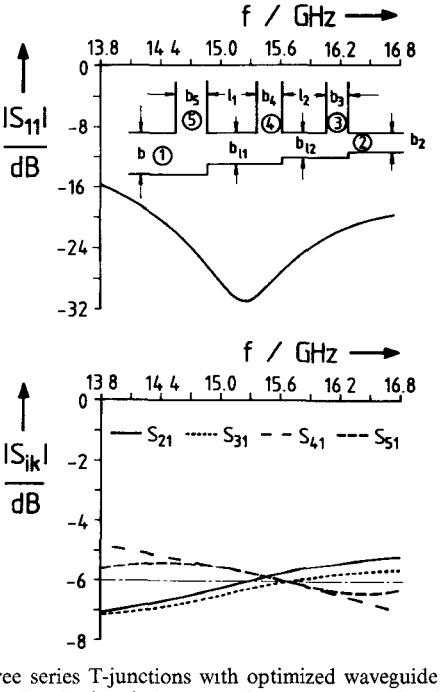

Fig. 6. Three series T-junctions with optimized waveguide heights and distances. Magnitude of the scattering coefficients in decibels as a function of frequency. Waveguide dimensions: $a = 2b = 15.799$ mm (R140-band); $b_2 = 3.41$ mm, $b_3 = 3.67$ mm, $l_2 = 7.94$ mm, $b_{12} = 3.96$ mm, $b_4 = 2.67$ mm, $l_1 = 7.95$ mm, $b_{l1} = 7.39$ mm, $b_5 = 2.65$ mm.

gether with about 28 dB return loss (Fig. 6). The five-series-T-junction type (Fig. 7) shows a higher deviation (about 1 dB) of the coupling response (-6.99 dB) at the ports. As may be shown by corresponding calculations, a

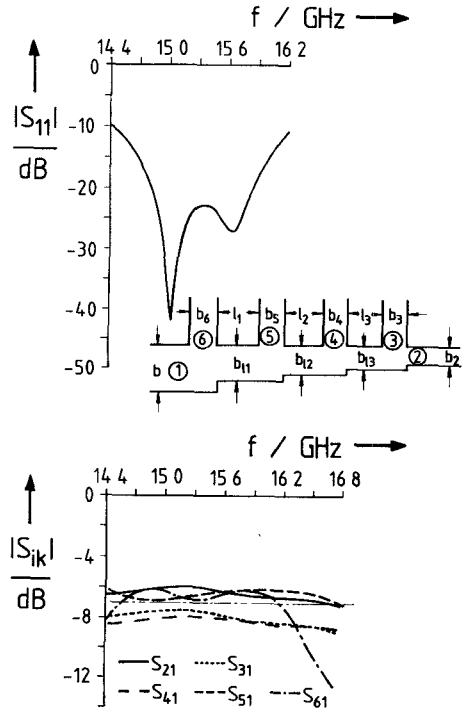

Fig. 7. Four series T-junctions with optimized waveguide heights and distances. Magnitude of the scattering coefficients in decibels as a function of frequency. Waveguide dimensions: $a = 2b = 15.799$ mm, $b_2 = 3.19$ mm, $b_3 = 2.52$ mm, $l_3 = 18.17$ mm, $b_{13} = 5.54$ mm, $b_4 = 2.52$ mm, $l_2 = 10.63$ mm, $b_{12} = 3.19$ mm, $b_5 = 7.33$ mm, $l_1 = 53.90$ mm, $b_{11} = 7.79$ mm, $b_6 = 1.90$ mm.

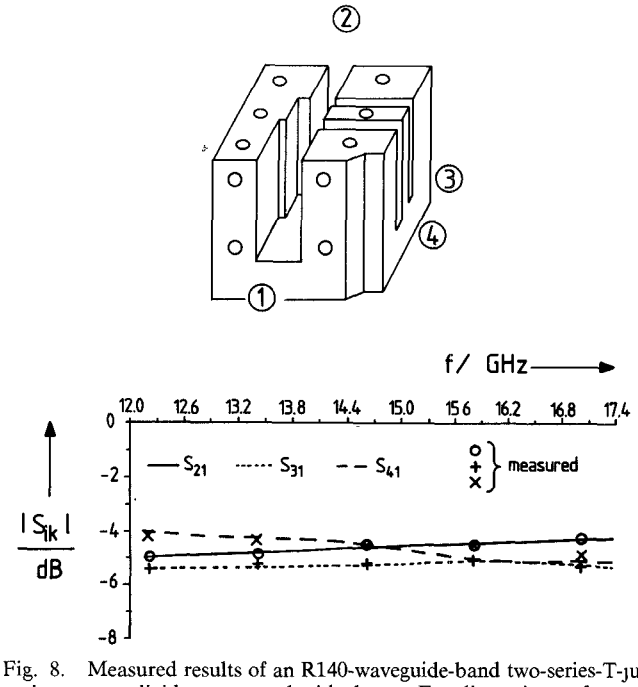

Fig. 8. Measured results of an R140-waveguide-band two-series-T-junction power divider compared with theory. For dimensions, cf. caption to Fig 5.

longer intermediate section l_2, instead of the 10.6 mm for the optimized compact design in Fig. 7, helps to reduce the mutual influence of the discontinuities and, hence, leads to reduced coupling deviation at the ports; the disadvantage of this design, however, is an increased overall length of the power divider.

Fig. 8 shows the measured results of an R140-waveguide-band two-series-T-junction power divider (−4.77 dB power division), which are compared with the theoretically predicted values. Convenient milling and spark eroding techniques may lead to a compact design. The optimized design data are given in the caption of Fig. 5. The measured results are in good agreement with the theory. The measured return loss at port 1 was typically about 30 dB between 12.8 and 16 GHz. Tapered transitions to standard R140-waveguide height dimensions ($b = 7.898$ mm) are connected to ports 4, 3, and 2, respectively.

V. Conclusions

Series *E*-plane T-junctions with different suitably optimized waveguide heights and distances achieve simple power dividers appropriate for compact topology. A suitable computer-aided design of such power dividers is based on direct modal expansion in scattered waves, which allows the inclusion of the effects of all step discontinuities and mutual higher order mode interaction. Convenient milling and spark eroding techniques permit low-cost mass production, since no additional matching elements, such as irises or posts, are necessary. Since all significant discontinuity and coupling effects are included in the design theory, measurements agree well with the theoretical predictions.

Appendix

Matrix Elements in (4):

$$(S_T) = \begin{bmatrix} -(e_1)(Y_1) & (Y_1) & -(T_1)(Y_3) \\ (Y_1) & -(e_1)(Y_1) & (T_2)(Y_3) \\ -(T_3)(Y_1) & (T_4)(Y_1) & -(e_3)(Y_3) \end{bmatrix}^{-1} * \begin{bmatrix} (1/e_1)(Y_1) & -(Y_1) & (T_1)(Y_3) \\ -(Y_1) & (1/e_1)(Y_1) & -(T_2)(Y_3) \\ (T_3)(Y_1) & -(T_4)(Y_1) & (1/e_3)(Y_3) \end{bmatrix} \quad \text{(A1)}$$

Coefficients of the Coupling Matrices (T_1), (T_2), (T_3), (T_4):

$$T_{1np} = \frac{1}{\sqrt{y_1 z_1}} \frac{\sin\left(\beta_n^{\mathrm{I}} 2z_1\right)}{\sin\left(\beta_p^{\mathrm{III}} 2z_1\right)} \frac{\beta_n^{\mathrm{I}}}{\beta_p^{\mathrm{III}}} \frac{1}{\sqrt{1+\delta_{0n}}} \frac{1}{\sqrt{1+\delta_{0p}}} * \int_{-y_1}^{y_1} \cos\left[\beta_p^{\mathrm{III}}(-y+y_1)\right] \cos\left[\frac{n\pi}{2y_1}(y+y_1)\right] dy \quad \text{(A2)}$$

$$T_{2np} = (-1)^p T_{1np} \quad \text{(A3)}$$

$$T_{3np} = \frac{1}{\sqrt{y_1 z_1}} \frac{\beta_p^{\mathrm{III}}}{\beta_n^{\mathrm{I}}} \frac{\sin\left(\beta_p^{\mathrm{III}} 2y_1\right)}{\sin\left(\beta_n^{\mathrm{I}} 2z_1\right)} \frac{1}{\sqrt{1+\delta_{0n}}} \frac{1}{\sqrt{1+\delta_{0p}}} * \int_{-z_1}^{z_1} \cos\left[\beta_n^{\mathrm{I}}(-z+z_1)\right] \cos\left[\frac{p\pi}{2z_1}(z+z_1)\right] dz \quad \text{(A4)}$$

$$T_{4np} = (-1)^p T_{3np}. \quad \text{(A5)}$$

Elements of the Diagonal Matrices (Y_I), (Y_3), (e_I), (e_3), $(1/e_I)$, $(1/e_3)$:

$$Y_{1n} = \frac{1}{\sqrt{Z^{\mathrm{I}}_{Fn}}} \qquad Y_{3n} = \frac{1}{\sqrt{Z^{\mathrm{III}}_{Fp}}} \tag{A6}$$

$$e_{1n} = \exp\left(j\beta^{\mathrm{I}}_n 2z_1\right) \qquad e_{3p} = \exp\left(j\beta^{\mathrm{III}}_p 2y_1\right)$$
$$1/e_{1n} = \exp\left(-j\beta^{\mathrm{I}}_n 2z_1\right) \qquad 1/e_{3p} = \exp\left(-j\beta^{\mathrm{III}}_p 2y_1\right)$$
$$Z_F\text{: cf. (2).} \tag{A7}$$

Submatrices in (5):

$$(S_{11}) = \left[\left(\sqrt{Y_m}\right)(1/\beta_m)\left[(K_{1nm})\left(\sqrt{Y_m}\right)\right]^{-1}\left(\sqrt{Y_n}\right) + (K_{2mn})(1/\beta_n)\left(\sqrt{Y_n}\right)\right]^{-1} * \left[-\left(\sqrt{Y_m}\right)(1/\beta_m)\left[(K_{1nm})\left(\sqrt{Y_m}\right)\right]^{-1}\left(\sqrt{Y_n}\right) + (K_{2mn})(1/\beta_n)\left(\sqrt{Y_n}\right)\right] \tag{A8}$$

$$(S_{12}) = 2\left[\left(\sqrt{Y_m}\right)(1/\beta_m)\left[(K_{1nm})\left(\sqrt{Y_m}\right)\right]^{-1}\left(\sqrt{Y_n}\right) + (K_{2mn})(1/\beta_n)\left(\sqrt{Y_n}\right)\right]^{-1}\left(\sqrt{Y_m}\right)(1/\beta_m) \tag{A9}$$

$$(S_{21}) = 2\left[(K_{1nm})\left(\sqrt{Y_m}\right) + \left(\sqrt{Y_n}\right)\left[(K_{2mn})(1/\beta_n)\left(\sqrt{Y_n}\right)\right]^{-1} * \left(\sqrt{Y_m}\right)(1/\beta_m)\right]^{-1}\left(\sqrt{Y_n}\right) \tag{A10}$$

$$(S_{22}) = \left[(K_{1nm})\left(\sqrt{Y_m}\right) + \left(\sqrt{Y_n}\right)\left[(K_{2mn})(1/\beta_n)\left(\sqrt{Y_n}\right)\right]^{-1} * \left(\sqrt{Y_m}\right)(1/\beta_m)\right]^{-1} * \left[-(K_{1nm})\left(\sqrt{Y_m}\right) + \left(\sqrt{Y_n}\right)\left[(K_{2mn})(1/\beta_n)\left(\sqrt{Y_n}\right)\right]^{-1} * \left(\sqrt{Y_m}\right)(1/\beta_m)\right]. \tag{A11}$$

Coefficients of the Coupling Matrices (K_1), (K_2):

$$K_{1nm} = \frac{1}{\sqrt{1+\delta_{0m}}} \cdot \frac{1}{\sqrt{1+\delta_{0n}}} \cdot \frac{2}{\sqrt{(y_1 - y_0)(y_2 - y_3)}} \cdot \int_{y_3}^{y_2} \cos\left[\frac{m\pi}{(y_1 - y_0)}(y - y_0)\right] \cos\left[\frac{n\pi}{y_2 - y_3}(y - y_3)\right] dy$$

$$(K_{2mn}) = (K_{1mn})'\,(' = \text{transposed}). \tag{A12}$$

Elements of the Diagonal Matrices $(\sqrt{Y_m})$, $(\sqrt{Y_n})$, $(1/\beta_m)$, $(1/\beta_n)$:

$$\left(\sqrt{Y_m}\right)_m = \frac{1}{\sqrt{Z^{\mathrm{V}}_{Fm}}} \qquad \left(\sqrt{Y_n}\right)_n = \frac{1}{\sqrt{Z^{\mathrm{IIa}}_{Fn}}}$$
$$(1/\beta_m)_m = 1/\beta^{\mathrm{V}}_m \qquad (1/\beta_n)_n = 1/\beta^{\mathrm{IIa}}_n. \tag{A13}$$

Submatrices of (6):

$$\begin{aligned}
(S^{UT}_{11}) &= (S^T_{11}) + (S^T_{12})(M_2)(S^T_{21}) \\
(S^{UT}_{12}) &= (S^T_{12})(S^H_{12}) + (S^T_{12})(M_2)(M_4) \\
(S^{UT}_{13}) &= (S^T_{13}) + (S^T_{12})(M_2)(S^T_{23}) \\
(S^{UT}_{21}) &= (M_3)(S^T_{21}) \\
(S^{UT}_{22}) &= (S^H_{22}) + (M_3)(M_4) \\
(S^{UT}_{23}) &= (M_3)(S^T_{23}) \\
(S^{UT}_{31}) &= (S^T_{31}) + (S^T_{32})(M_2)(S^T_{21}) \\
(S^{UT}_{32}) &= (S^T_{32})(S^H_{12}) + (S^T_{32})(M_2)(M_4) \\
(S^{UT}_{33}) &= (S^T_{33}) + (S^T_{32})(M_2)(S^T_{23})
\end{aligned} \tag{A14}$$

with the abbreviations

$$\begin{aligned}
(M_2) &= (S^H_{11})(M_1) \\
(M_3) &= (S^H_{21})(M_1) \\
(M_4) &= (S^T_{22})(S^H_{12}) \\
(M_1) &= \left[(U) - (S^T_{22})(S^H_{11})\right]^{-1}
\end{aligned}$$

(U): unit matrix.

Equivalent-Circuit Parameters (Fig. 2):

$$YC = Y_{23} = -Y_{13} \qquad YD = Y_{33} - Y_{23}$$
$$YB = -Y_{21} - Y_{23} \qquad YA = Y_{11} + Y_{21} \tag{A15}$$

where the matrix elements of (Y) are calculated by (7) utilizing the rigorous field theory method.

Acknowledgment

The authors thank Dr. Bätz, Dr. Meck, and Dr. Fasold for helpful discussions.

References

[1] N. Marcuvitz, *Waveguide Handbook*. New York: McGraw-Hill, 1951, chs. 6 and 7.
[2] A. Rogers, "Wideband squintless linear arrays," *Marconi Rev.*, vol. 35, no. 187, 1972.
[3] C. G. Cox, "An analysis of the waveguide squintless feed," *Marconi Rev.*, vol. 44, no. 222, 1981.
[4] C. G. Cox, "Waveguide power divider for satellite use," in *Proc. 3rd Int. Conf. Antennas Propagat.* (Norwich, England), 1983, pp. 341–343.
[5] P. J. Meier, "Integrated finline: The second decade," *Microwave J.*, vol 28, no 11, pp. 31–54, Nov. 1985; also no. 12, pp. 30–48, Dec. 1985.
[6] K. Solbach, "The status of printed millimeter-wave *E*-plane circuits," *IEEE Trans. Microwave Theory Tech*, vol. MTT-31, pp. 107–121, Feb. 1983.
[7] F Arndt, J. Bornemann, D. Grauerholz, D. Fasold, and N. Schröder, "Waveguide *E*-plane integrated circuit diplexers," *Electron. Lett.*, vol. 21, pp. 615–617, July 1985.
[8] R. Levy, "Analysis of practical branch-guide directional couplers," *IEEE Trans. Microwave Theory Tech.*, vol. MTT-17, pp. 289–290, May 1969.
[9] R. Levy, "Zolotarev branch-guide couplers," *IEEE Trans. Microwave Theory Tech*, vol. MTT-21, pp. 95–99, Feb. 1973.
[10] E. D. Sharp, "An exact solution for a T-junction of rectangular waveguide having arbitrary cross sections," *IEEE Trans. Microwave Theory Tech.*, vol. MTT-15, pp. 109–116, Feb. 1967.

[11] W. Bräckelmann, "Hohlleiter-Verbindungen für Rechteckhohlleiter," *Nachrichtentech. Z.*, vol. 22, pp. 2–7, Jan. 1970.
[12] E. Kühn, "A mode-matching method for solving field problems in waveguide and resonator circuits," *Arch. Elek. Übertragung.*, vol. 27, pp. 511–518, Dec. 1973.
[13] F. Arndt, B. Koch, H.-J. Orlock, and N. Schröder, "Field theory design of rectangular waveguide broadwall metal insert slot couplers for millimeter-wave applications," *IEEE Trans. Microwave Theory Tech.*, vol. MTT-33, pp. 95–104, Feb. 1985.
[14] F. Arndt, U. Tucholke, and T. Wriedt, "Computer-optimized multisection transformers between rectangular waveguides of adjacent frequency bands," *IEEE Trans. Microwave Theory Tech.*, vol. MTT-32, pp. 1479–1484, Nov. 1984.
[15] R. E. Collin, *Field Theory of Guided Waves*. New York: McGraw-Hill, 1960, pp. 338–348, 171–179, 85–87.
[16] R. F. Harrington, *Time Harmonic Electromagnetic Fields*. New York: McGraw-Hill, 1961, pp. 171–177.
[17] K. Kurokawa, "The expansion of electromagnetic fields in cavities," *IRE Trans. Microwave Theory Tech.*, vol. MTT-6, pp. 178–187, Feb. 1958.
[18] H. Patzelt and F. Arndt, "Double-plane steps in rectangular waveguides and their applications for transformers, irises, and filters," *IEEE Trans. Microwave Theory Tech.*, vol. MTT-30, pp. 771–776, May 1982.
[19] H. Schmiedel, "Anwendung der Evolutionsoptimierung bei Mikrowellenschaltungen," *Frequenz*, vol. 35, pp. 306–310, Nov. 1981.
[20] G. L. Matthaei, L. Young, and E. M. T. Jones, *Microwave Filters, Impedance-Matching Networks, and Coupling Structures*. New York: McGraw-Hill, 1964, p. 837.

Fritz Arndt (SM'83) was born in Konstanz, Germany, on April 30, 1938. He received the Dipl. Ing., Dr. Ing., and Habilitation degrees from the Technical University of Darmstadt, Germany, in 1963, 1968, and 1972, respectively.

From 1963 to 1973, he worked on directional couplers and microstrip techniques at the Technical University of Darmstadt. Since 1972, he has been a Professor and Head of the Microwave Department of the University of Bremen, Germany. His research activities are in the area of the solution of field problems of waveguide, finline, and optical waveguide structures, of antenna design, and of scattering structures.

Dr. Arndt is a member of the VDE and NTG (Germany). He received the NTG award in 1970, the A. F. Bulgin Award (together with three coauthors) from the Institution of Radio and Electronic Engineers in 1983, and the best paper award of the antenna conference JINA 1986 (France).

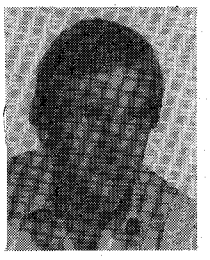

Ingo Ahrens was born in Oldenburg, West Germany, on September 9, 1958. He received the Dipl. Ing. degree in electrical engineering from the University of Bremen in 1984.

Since 1985 he has been working at MBB/Erno—Space Systems Group—in Bremen as a systems engineer, responsible for electrical systems on satellites and spacecraft.

Uwe Papziner was born in Delmenhorst, West Germany, on January 18, 1961. He received the Dipl. Ing. degree in electrical engineering from the University of Bremen, West Germany, in June 1986.

Since September 1986 he has been a Scientific Assistant at the University of Bremen, working on waveguide filter and multiplexer design problems.

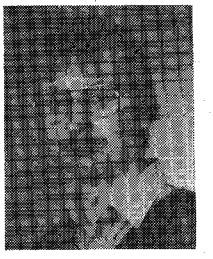

Ulrich Wiechmann was born in Bremen, West Germany, on February 14, 1959. He received the Dipl. Ing. degree in electrical engineering from the University of Bremen in 1984.

Since 1985 he has been working at Messerschmitt-Bölkow-Blohm in Bremen as a systems engineer responsible for electronic systems for center-of-gravity control in civil aircraft.

Reinhard Wilkeit was born in Bremerhaven, West Germany, on October 6, 1954. He received the Dipl. Ing. degree from the University of Bremen, Wester Germany, in 1984.

Since 1985 he has been with the ERNO Raumfahrttechnik GmbH, Bremen, where he works on flight operations.